Journal of Alloys and Compounds 489 (2010) 499–503

Contents lists available at ScienceDirect

Journal of Alloys and Compounds

journal homepage: www.elsevier.com/locate/jallcom

Magnetic property enhancement of directly quenched Nd–Fe–B bulk magnets with Ti substitution

H.W. Chang[a,*], M.F. Shih[b], C.C. Hsieh[b], W.C. Chang[b], C.Y. Shen[c]

[a] Department of Physics, Tunghai University, Taichung 407, Taiwan, ROC
[b] Department of Physics, National Chung Cheng University, Chia-Yi 621, Taiwan, ROC
[c] Department of Electrical Engineering, Hsiuping Institute of Technology, Taichung 412, Taiwan, ROC

ARTICLE INFO

Article history:
Received 5 August 2009
Received in revised form 8 September 2009
Accepted 9 September 2009
Available online 25 September 2009

PACS:
74.25.Ha
75.50.Vv
75.50.Ww

Keywords:
Hard magnetic material
Copper mold casting
Magnetic properties

ABSTRACT

Magnetic properties, phase evolution, and microstructure of directly quenched $Nd_yFe_{85-x-y}Ti_xB_{15}$ (x = 0–4; y = 8–10) bulk magnetic rods with a diameter of 0.7 mm were studied. The experimental results show that Ti substitution can not only suppress the formation of the $Nd_2Fe_{23}B_3$ and one unknown phases, leading to the presence of the large amount of $Nd_2Fe_{14}B$ phase, but also refine the grain size, resulting in the remarkable enhancement of magnetic properties. Besides, proper Ti substitution and Nd concentration can well modify phase constitution and uniformly refine grain size. In this study, the optimal magnetic properties of B_r = 6.5 kG, $_iH_c$ = 10.3 kOe and $(BH)_{max}$ = 8.7 MGOe are achieved in $Nd_{9.5}Fe_{72.5}Ti_3B_{15}$ magnet.

1. Introduction

In the R–Fe–B system, two different types of nanocomposites magnets, $R_2Fe_{14}B/\alpha$-Fe and $R_2Fe_{14}B/Fe_3B$, have been widely developed via melt spinning for bonded magnet applications, because their remanence B_r and maximum energy product $(BH)_{max}$ can be effectively enhanced by exchange coupling effect between magnetically soft and hard phases [1–8]. Traditionally, the bonded magnets have been produced from molding the powders, obtained by combining the crushing melt spun ribbons, fabricated at an optimal quenching velocity and followed by post-annealing with proper temperature, with a polymer binder. The main disadvantages of the traditional method include multifarious manufacturing processes and the dilution of magnetic properties by nonmagnetic polymer.

To overcome these disadvantages, a new group of R–Fe–M–B (R = Pr, Pr + Dy, Nd + Dy; M = Co, Cu, Mo, Nb, Ti, V, and Zr) bulk metallic glasses have been developed by copper mold casting method, and then followed by one-step heat treatment to optimize the permanent magnetic properties [9–13]. The compositions with the extremely high B content, such as $R_{3-4.5}Fe_{bal.}M_xB_{20}$ (R = Pr, Pr + Dy, Nd + Dy; M = Co, Cu, Mo, Nb, Ti, V, and Zr), were adopted in order to produce bulk amorphous precursor in rod form with 0.5–0.6 mm in diameter at first, and then they were annealed at 600–700 °C for 10–30 min [9–13]. Although higher $(BH)_{max}$ of 7.3–12.0 MGOe can be attained, the intrinsic coercivity ($_iH_c$) is too low (<4 kOe), resulting from the existence of considerable amount of the magnetically soft phases α-Fe or Fe_3B, to suit for high temperature application. Zhang et al. reported that after optimal crystallization, the bulk $Nd_{9.6}Fe_{bal.}Nb_4B_{22.08}$ alloy showed a high coercivity of 13.8 kOe but a relatively low $(BH)_{max}$ (~4 MGOe) [14], and Tan et al. reported that $Nd_5Y_4Fe_{68}Zr_2B_{21}$ bulk sheet specimens with relatively larger size of $0.8 \times 10 \times 50\,mm^3$, annealed at 690 °C, exhibited ordinary magnetic properties of $_iH_c$ = 4.8 kOe and $(BH)_{max}$ = 5.4 MGOe [15].

In our previous study [16–18], for melt spinning ribbons, the R-lean and B-enriched $R_{8-11}Fe_{bal.}M_2B_{10-15}$ with Ti substitution exhibits high coercivity ($_iH_c$) and $(BH)_{max}$ simultaneously, because proper volume fraction of magnetically soft and hard phases and uniformly fine grains are obtained in them. To explore the possibility of simplifying manufacturing process for making isotropic magnet, in this study, we adopt the copper mold casting method to fabricate directly quenched bulk NdFeTiB magnet, in the rod form of a larger diameter of 0.7 mm, without any post-heat treatment. The effects of Ti and Nd contents on the magnetic properties and microstructure of directly quenched $Nd_yFe_{85-x-y}Ti_xB_{15}$ (x = 0–4; y = 8–10) bulk magnets are reported.

* Corresponding author. Tel.: +886 4 23594643; fax: +886 4 23594643.
E-mail address: wei0208@gmail.com (H.W. Chang).

0925-8388/$ – see front matter © 2009 Published by Elsevier B.V.
doi:10.1016/j.jallcom.2009.09.094

2. Experimental

Alloy ingots with nominal compositions of $Nd_yFe_{85-x-y}Ti_xB_{15}$ (x = 0–4; y = 8–10) were prepared by arc melting mixtures of pure Nd, Fe, and M metal and pure B crystal in an argon atmosphere. 5% excess Nd was adopted to compensate the loss of Nd during processing. These magnetic rods with cylindrical shape of a diameter of 0.7 and 15 mm in length were obtained by injection casting into a copper mold. The Curie temperatures of magnetic phases were determined by a thermal gravimetric analyzer (TGA) with an externally applied magnetic field (conventionally referred as "TMA"), under a heating rate of 20 °C/min. The macroscopic morphology of the cross-section of rods was studied using a scanning electron microscopy (SEM), while the microstructure was directly observed by a transmission electron microscopy (TEM). The crystalline structures of the powders, crushed from the bulk rods, were identified by X-ray powder diffraction (XRD) with Cu-Kα radiation. The magnetic properties of the rods at room temperature were measured by a vibrating sample magnetometer (VSM). All samples were magnetized by a 50 kOe peak pulse field prior to magnetic measurement. For the cylinder samples with a diameter of 0.7 mm and a length of about 3 mm, the proper factor of 0.7 is applied to correct demagnetization.

3. Results and discussion

At first, effect of Ti content on the magnetic properties and phase evolution of directly quenched $Nd_{9.5}Fe_{75.5-x}Ti_xB_{15}$ (x = 0–4) magnets have been studied. Fig. 1 shows the second quadrant demagnetization curves of $Nd_{9.5}Fe_{75.5-x}Ti_xB_{15}$ alloys. Obviously, the ${}_iH_c$ of the alloy rod increase from 1.0 kOe for x = 0 to extremely high value of 13.4 kOe for x = 2, however, due to the lower B_r and poor squareness of the demagnetization curve (SQ), the magnetic energy product of the latter is as high as 7.0 MGOe. Interestingly, as the Ti content x is increased to 3, the coercivity is slightly decreased to 10.3 kOe, but the remanence and the SQ are improved, giving rise to the highest magnetic energy product (8.7 MGOe) in this series alloys. Further increase of x to 3.5 or 4, the remanence does not increase, instead, ${}_iH_c$ continues to decrease, degrading the magnetic energy product to 8.0 and 7.7 MGOe for x = 3.5 and 4, respectively.

Fig. 2 shows X-ray diffraction patterns of directly quenched $Nd_{9.5}Fe_{75.5-x}Ti_xB_{15}$ bulk magnets. For all the samples, almost all diffraction peaks of $Nd_2Fe_{14}B$ phase are overlapped with those of $Nd_2Fe_{23}B_3$, Fe_3B, α-Fe, or other existed phase to complicate the phase identification. Nevertheless, it is seen that the full width at half of the maximum (FWHM) for diffraction peaks slightly become broadened with Ti substitution, and the average grain size, estimated from XRD analysis based on the Scherrer's formula, is reduced with Ti substitution from 55.2 nm for x = 0 to 24.5–41.5 nm for x = 1–4. Besides, almost all diffraction peaks for 2:14:1 phase slightly shifts toward lower angle side, indicating that a part of Ti elements have entered the crystal structure of 2:14:1 phase to form $Nd_2(Fe,Ti)_{14}B$ phase due to the larger atomic radius of Ti (0.147 nm) than that of Fe (0.124 nm).

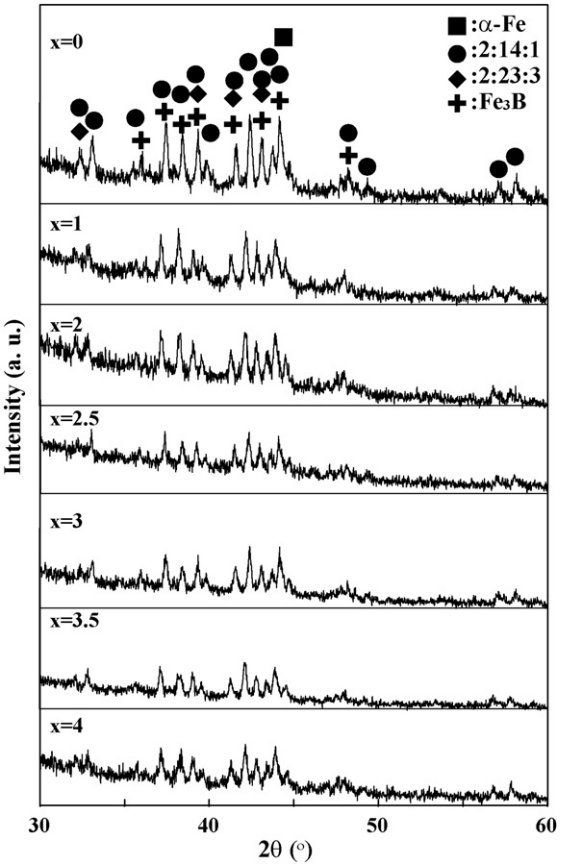

Fig. 2. XRD patterns of directly quenched $Nd_{9.5}Fe_{75.5-x}Ti_xB_{15}$ bulk magnets.

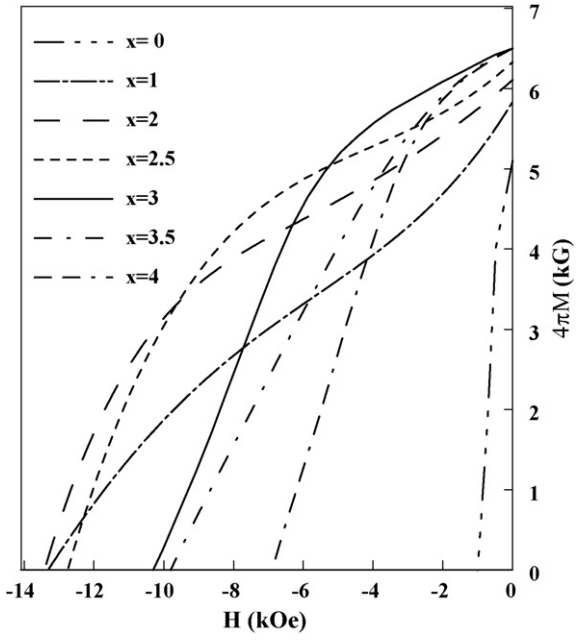

Fig. 1. Demagnetization curves of directly quenched $Nd_{9.5}Fe_{75.5-x}Ti_xB_{15}$ bulk magnets with a diameter of 0.7 mm.

To understand magnetic phase constitution of directly quenched $Nd_{9.5}Fe_{75.5-x}Ti_xB_{15}$ bulk magnets, TMA technique is adopted. Fig. 3 presents TMA scans of directly quenched $Nd_{9.5}Fe_{75.5-x}Ti_xB_{15}$ bulk magnets with a diameter of 0.7 mm. For ternary $Nd_{9.5}Fe_{75.5}B_{15}$ magnet, in addition to $Nd_2Fe_{14}B$, $Nd_2Fe_{23}B_3$, Fe_3B, and α-Fe, an unknown phase with $T_C \sim 580$ °C is found. Clearly, magnetically soft 2:23:3 and unknown phases are suppressed to induce the presence of large volume fraction of $Nd_2Fe_{14}B$ phase, for the magnets with Ti substitution, resulting in the remarkable increase of coercivity from 1.7 kOe for x = 0 to 13.4 kOe for x = 2. However, the volume fraction of Fe_3B phase increases with the increase of Ti substitution, leading to the enhancement of remanence from 5.0 kG for x = 0 to 6.5 kG for x = 4, and also the gradual decrease of coercivity from 13.4 kOe for x = 2 to 6.9 kOe for x = 4. The increment of the amount of Fe_3B phase with the increase of Ti content might be presumed that more Ti substitution for Fe in this alloy system makes 2:14:1 phase more unstable. Furthermore, it is found that with the increment of x the Curie temperature (T_C) of 2:14:1 phase is decreased from 316 °C for x = 0 to 304 °C for x = 4, revealing that a part of Ti elements have entered the crystal structure of 2:14:1 phase, consistent with the outcome of XRD analysis.

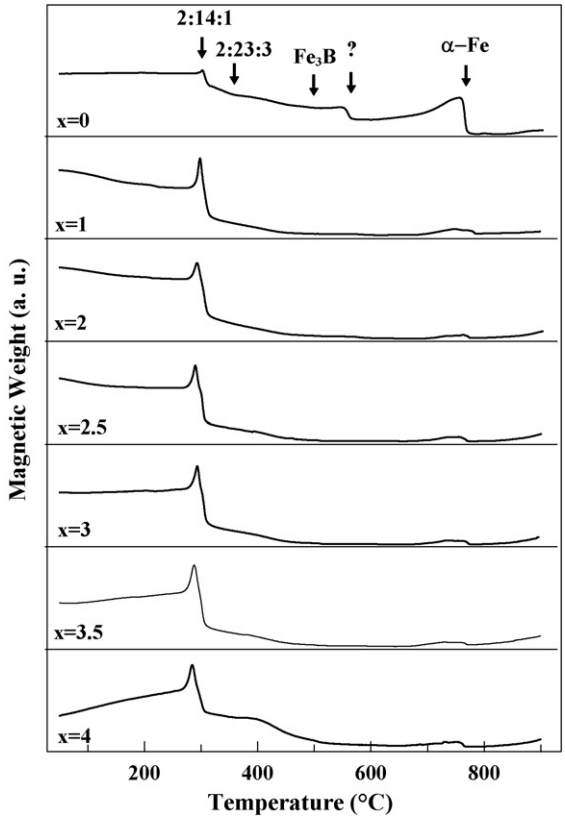

Fig. 3. TMA scans of directly quenched $Nd_{9.5}Fe_{75.5-x}Ti_xB_{15}$ bulk magnets.

Furthermore, effect of Nd content on the magnetic properties and phase evolution of directly quenched $Nd_yFe_{82-y}Ti_3B_{15}$ (y = 8–10) magnets is also studied. Fig. 4 shows their second quadrant demagnetization curves, and magnetic properties are summarized to list in Table 1. Clearly, with the decrease of Nd content y, B_r slightly increases from 6.4 kG for y = 10 to 6.5 kG for y = 9–9.5 at first, and then decreases to 5.8 kG for y = 8, on the contrary, $_iH_c$ decreases monotonously from 11.8 kOe for y = 10 to 6.7 kOe for y = 8. On the other hand, SQ is deteriorated with decreasing y from 9.5 to 8. Therefore, with the decrease of Nd content, $(BH)_{max}$ slightly increases from 8.6 MGOe for y = 10 to reach the maximum value of 8.7 MGOe for y = 9.5 at first, and then decreases to 4.1 MGOe for y = 8. This suggests that proper Nd content is important to obtain the directly quenched $Nd_yFe_{82-y}Ti_3B_{15}$ magnets with higher both $_iH_c$ and $(BH)_{max}$. In these studied alloys, the optimal magnetic properties of B_r = 6.5 kG, $_iH_c$ = 10.3 kOe and $(BH)_{max}$ = 8.7 MGOe are achieved in $Nd_{9.5}Fe_{72.5}Ti_3B_{15}$ magnet. It is worthy to note that the directly quenched $Nd_yFe_{82-y}Ti_3B_{15}$ rods with a diameter of 0.7 mm could exhibit high coercivity and energy product simultaneously.

Table 1
Magnetic properties of directly quenched $Nd_yFe_{82-y}Ti_3B_{15}$ bulk magnets with a diameter of 0.7 mm.

y	B_r (kG)	$_iH_c$ (kOe)	$(BH)_{max}$ (MGOe)
10	6.4	11.8	8.6
9.5	6.5	10.3	8.7
9	6.5	8.7	7.7
8.5	6.1	8.3	5.7
8	5.8	6.7	4.1

Fig. 5 presents TMA scans of $Nd_yFe_{82-y}Ti_3B_{15}$ bulk magnets. It is found that the large volume fraction of magnetically hard 2:14:1 phase coexists with minor amount of soft Fe_3B and α-Fe phase in this series magnetic rod. In addition, the volume fraction of 2:14:1 phase decreases with decreasing Nd content, giving rise to a reduction of $_iH_c$, and it is in agreement with our previous study of $Pr_yFe_{88-y}Ti_2B_{10}$ (y = 7–9.5) nanocomposite ribbons [17]. Furthermore, magnetically metastable 2:23:3 phase appears for the rod with y = 8.5, resulting in the marked reduction of remanence and the deterioration of SQ, and besides, due to the presence of amorphous phase, the demagnetization curves with the shoulder phenomenon occurs for the magnet with lower Nd content of 8 at%, as shown in Fig. 4, resulting in the deterioration of magnetic properties.

From the macroscopic study, with SEM of the cross-section of bulk magnets, the morphology normally consists of a fine grained peripheral region and a coarse grained core region. The latter has a typical dendritic microstructure, and the area is verified with the

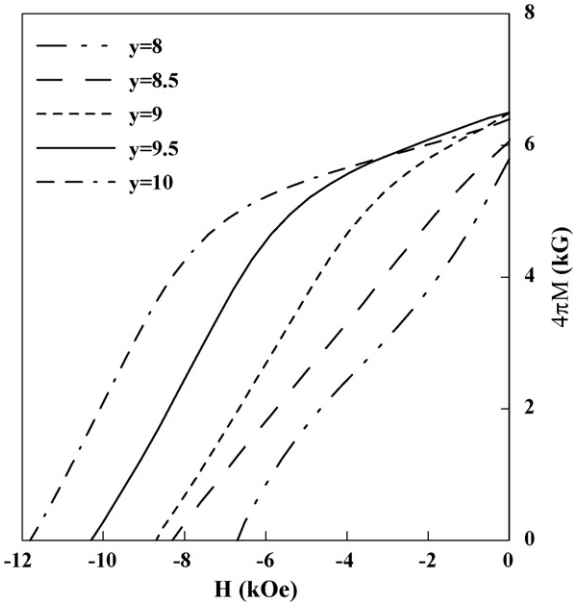

Fig. 4. Demagnetization curves of directly quenched $Nd_yFe_{82-y}Ti_3B_{15}$ bulk magnets.

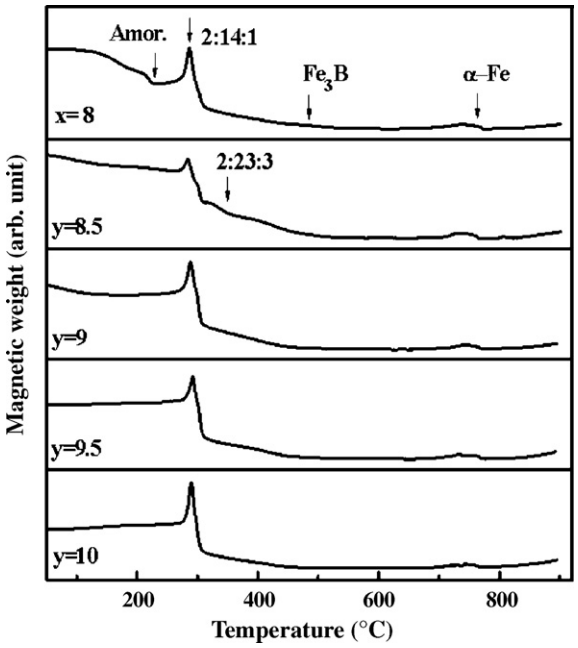

Fig. 5. TMA scans of directly quenched $Nd_yFe_{82-x}Ti_3B_{15}$ bulk magnets.

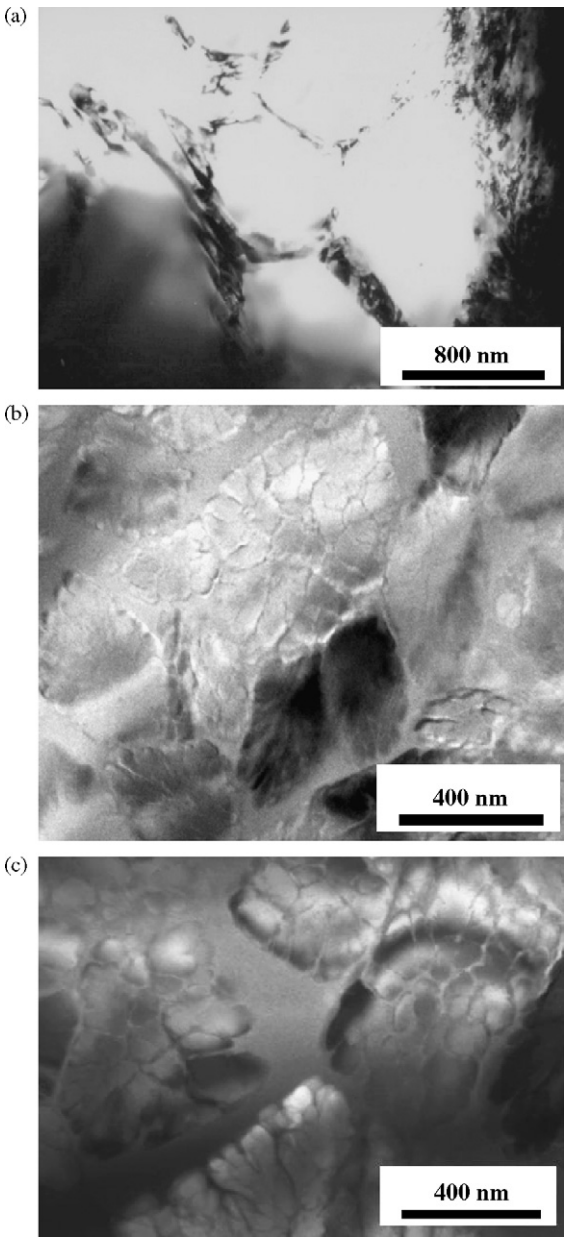

Fig. 6. TEM images of directly quenched (a) $Nd_{9.5}Fe_{75.5}B_{15}$, (b) $Nd_{9.5}Fe_{72.5}Ti_3B_{15}$, and (c) $Nd_8Fe_{74}Ti_3B_{15}$ bulk magnets.

transition metals adopted. It is in contrast to the morphology that observed in the samples with 20 at% B [9–10]. Since the grain size and distribution of the magnets are very crucial to affect the $_iH_c$, SQ and the $(BH)_{max}$, it is needed to know the grain size especially at the core region of the magnets. Fig. 6(a–c) depicts TEM images of the core region of directly quenched $Nd_{9.5}Fe_{75.5}B_{15}$, $Nd_{9.5}Fe_{72.5}Ti_3B_{15}$, and $Nd_8Fe_{74}Ti_3B_{15}$ magnets, respectively. Obviously, the grain size of ternary $Nd_{9.5}Fe_{75.5}B_{15}$ magnet is extremely large and can be estimated to 500–800 nm, however, substituting Ti for Fe is helpful in refining the grain size of the magnetic rod to 80–150 nm, respectively. Because of the slowest cooling rate for the core region of rod, the grain size of core region of rod, observed by TEM, is much larger than the average grain size, analyzed by XRD. Besides, grain boundary phase is observed for these samples, and it is more obvious for Ti-substituted ribbons. For identifying the composition of the grain boundary phase for Ti-substituted alloys, energy dispersive X-ray analysis (EDX) is employed. The EDX result shows that

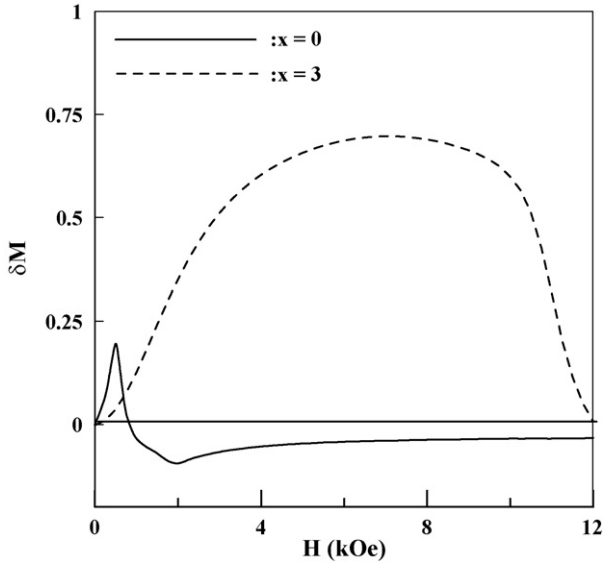

Fig. 7. Delta M curves of Ti-free $Nd_{9.5}Fe_{75.5}B_{15}$ and Ti-containing $Nd_{9.5}Fe_{72.5}Ti_3B_{15}$ bulk magnets.

Ti atom tends to appear at the grain boundary for Ti-substituted ribbons. It is presumed that Ti prefers to react with excess boron to form Ti-boride in the grain boundary, giving rise to the strong affinity between Ti and B. The isolation effect of nonmagnetic grain boundary phase is very beneficial in enhancing the coercivity of magnet [19].

Fig. 7 depicts the applied magnetic field dependence of $\delta M = m_d(H) - (1 - 2m_r(H))$ [20,21], with m_d being the reduced magnetization and m_r the reduced remanence, of Ti-free $Nd_{9.5}Fe_{75.5}B_{15}$, and Ti-containing $Nd_{9.5}Fe_{72.5}Ti_3B_{15}$ bulk magnets. The positive δM peak height, $(\delta M)_{max}$, indicates that the strength of exchange–coupling interaction between magnetic grains. Clearly, the exchange coupling effect exists in those two samples, and the stronger exchange coupling effect exists for Ti-containing $Nd_{9.5}Fe_{72.5}Ti_3B_{15}$ bulk magnets. The much larger $(\delta M)_{max}$ for Ti-containing $Nd_{9.5}Fe_{72.5}Ti_3B_{15}$ bulk magnets is mainly contributed by the strong exchange coupling effect between magnetically hard phases (2:14:1 phase) and soft phase (Fe_3B, and α-Fe phase) due to grain refinement with Ti substitution, leading to an enhancement in the remanence. Therefore, the main reasons for high magnetic property achieved in this studied alloy rods include proper volume fraction of magnetically soft and hard phases (2:14:1, Fe_3B, and α-Fe), fine grains, and grain boundary phase due to proper Ti substitution and Nd concentration.

4. Conclusions

Magnetic properties of directly quenched $Nd_yFe_{85-x-y}Ti_xB_{15}$ bulk magnets are dominated by phase constitution and microstructure. The Ti substitution for Fe in $Nd_{9.5}Fe_{75.5}M_xB_{15}$ alloy rod can not only suppress the formation of $Nd_2Fe_{23}B_3$ and one unknown phase, leading to the presence of the large volume fraction of $Nd_2Fe_{14}B$ phase, but also refine the grain size. Besides, proper Nd concentration can well modify phase constitution. As a result, the magnetic properties of the bulk magnetic rods are remarkably improved. In this study, $Nd_{9.5}Fe_{72.5}Ti_3B_{15}$ magnetic rods exhibit the best magnetic properties (B_r = 6.5 kG, $_iH_c$ = 10.3 kOe, and $(BH)_{max}$ = 8.7 MGOe). High magnetic properties are presumably resulted from proper phase constitutions, fine grains, and grain boundary phase.

Acknowledgements

This paper was supported by National Science Council, Taiwan under grant no. NSC-95-2112-M-194-009-MY3 and NSC-98-2112-M-029-001-MY3.

References

[1] R. Coehoorn, D.B. DeMooij, C. DeWaard, J. Magn. Magn. Mater. 80 (1989) 101.
[2] A. Manaf, R.A. Buckley, H.A. Davis, M. Leonowicz, J. Magn. Magn. Mater. 101 (1991) 360.
[3] Eckart F. Kneller, Reinhard Hawig, IEEE Trans. Magn. 27 (1991) 3588.
[4] H. Kanekiyo, M. Uehara, S. Hirosawa, IEEE Trans. Magn. 29 (1993) 2863.
[5] J. Bauer, M. Seeger, A. Zern, H. Kronmüller, J. Appl. Phys. 80 (1996) 1667.
[6] K. Raviprsad, M. Funakoshi, M. Umemoto, J. Appl. Phys. 83 (1998) 921.
[7] W.C. Chang, D.Y. Chiou, S.H. Wu, B.M. Ma, C.O. Bounds, Appl. Phys. Lett. 72 (1998) 121.
[8] W.C. Chang, S.H. Wu, B.M. Ma, C.O. Bounds, S.Y. Yao, J. Appl. Phys. 83 (1998) 2147.
[9] Wei Zhang, Akihisa Inoue, Appl. Phys. Lett. 80 (2002) 1610.
[10] Wei Zhang, Akihisa Inoue, J. Appl. Phys. 91 (2002) 8834.
[11] P. Pawlik, H.A. Davies, Scripta Mater. 49 (2003) 755.
[12] M. Marinescu, P.C. Pawlik, H.A. Davies, H. Chiriac, J. Optoelectron. Adv. Mater. 6 (2004) 603.
[13] M. Marinescu, H. Chiriac, M. Grigoras, J. Magn. Magn. Mater. 290 (2005) 1267.
[14] J. Zhang, K.Y. Kim, Y.P. Feng, Y. Li, Scripta Mater. 56 (2007) 943.
[15] Xiaohua Tan, Hui Xu, Qin Bai, Yuanda Dong, Appl. Phys. Lett. 91 (2007) 252501.
[16] H.W. Chang, C.H. Chiu, W.C. Chang, Appl. Phys. Lett. 82 (2003) 4513.
[17] C.H. Chiu, H.W. Chang, C.W. Chang, W.C. Chang, IEEE Trans. Magn. 41 (2005) 3769.
[18] H.W. Chang, C.H. Chiu, C.W. Chang, W.C. Chang, A.C. Sun, Y.D. Yao, Scripta Mater. 55 (2006) 529.
[19] Er. Girt, M. Kannan, G. Krishnan, Z. Thomas, Altounian, Appl. Phys. Lett. 76 (2000) (1746).
[20] P.E. Kelly, K. O'Grady, P.I. Mayo, R.W. Cantrell, IEEE Trans. Magn. 25 (1989) 388.
[21] F. Vajda, E.D. Torre, J. Appl. Phys. 75 (1994) 5689.